Open Journal of Applied Sciences, 2024, 14, 243-266
https://www.scirp.org/journal/ojapps
ISSN Online: 2165-3925
ISSN Print: 2165-3917

Simulation of Steel Reinforcement on the Nonlinear Behaviour of Slender Glulam Beam Columns by Using the Newton-Raphson Method

Martial Ourmama*, Marcelline Blanche Manjia, Edmond Dawak Fezeu

Laboratory of Civil Engineering and Mechanics, Department of Civil Engineering, National Advanced School of Engineering at Yaounde, The University of Yaounde I, Yaounde, Cameroon

Email: *ourmamamartial@hotmail.fr

How to cite this paper: Ourmama, M., Manjia, M.B. and Fezeu, E.D. (2024) Simulation of Steel Reinforcement on the Nonlinear Behaviour of Slender Glulam Beam Columns by Using the Newton-Raphson Method. *Open Journal of Applied Sciences*, **14**, 243-266.
https://doi.org/10.4236/ojapps.2024.142018

Received: November 18, 2023
Accepted: February 6, 2024
Published: February 9, 2024

Abstract

The current theory in NF EN 1995-1-1/NA of Eurocode 5, which is based on maximum deflection, has been investigated on softwoods. Therefore, this theory is not adapted for slender glulam beam columns made of tropical hardwood species from the Congo Basin. This maximum deflection is caused by a set of loads applied to the structure. However, Eurocode 5 doesn't provide how to predict this deflection in case of long-term load for such structures. This can be done by studying load-displacement (P-Δ) behaviour of these structures while taking into account second order effects. To reach this goal, a nonlinear analysis has been performed on a three-dimensional beam column embedded on both ends. Since conducting experimental investigations on large span structural products is time-consuming and expensive especially in developing countries, a numerical model has been implemented using the Newton-Raphson method to predict load-displacement (P-Δ) curve on a slender glulam beam column made of tropical hardwood species. On one hand, the beam has been analyzed without wood connection. On the other hand, the beam has been analyzed with a bolted wood connection and a slotted-in steel plate. The load cases considered include self-weight and a uniformly applied long-term load. Combinations of serviceability limit states (SLS) and ultimate limit states (ULS) have also been considered, among other factors. A finite-element software RFEM 5 has been used to implement the model. The results showed that the use of steel can reduce displacement by 20.96%. Additionally, compared to the maximum deflection provided by Eurocode 5 for softwoods, hardwoods can exhibit an increasing rate of 85.63%. By harnessing the plastic resistance of steel, the bending resistance of wood can be increased by 32.94%.

Keywords

Nonlinear Analysis, Newton-Raphson Method, Maximum Deflection, Bolted Wood Connection, Hardwood Species

1. Introduction

Slender glulam beam columns are mostly used in civil engineering constructions such as bridges and multi-storey buildings. The use of wood, as a structural main-based material in such infrastructures, may present several advantages. It is aesthetic and endowed with an interesting strength-to-weight ratio compared to materials such as concrete and steel [1]. Construction wood fares well in environmental analyses due to its carbon sequestration properties and the climate benefits associated with the sustainable management of forests [2]. However, in practice high rise constructions only made of wood is almost impossible [3]. It is convenient to insert some steel-wood connection members such as dowels, screws, bolts etc. In this case, the connection should be strong enough to transmit shear loads developed in the interface and rigid enough to limit slip between wood and steel. Therefore, the mechanical behaviour of the connection has a significant importance in the behaviour of the composite structures, not only in the stresses but also in the deformations [4].

The analysis of the connection behaviour can be performed using numerical models or laboratory tests. In order to study the mechanical behaviour of bolted wood connections, three-dimensional (3D) constitutive models were developed in [5] for wood, adapted to a 3D finite element (FE) numerical model of a bolted wood connection. A nonlinear parallel-to-grain compression of wood was performed to predict load-displacement (P-Δ) curve in bolted wood connections. The numerical results matched well with the experimental results. However, in the numerical implementation of their models, 3D nonlinear orthotropic material constitutive behaviour was not considered. Furthermore, bending strength which can lead to large deformations was not considered. A two-dimensional FE model was used in [6] to assess the plywood reinforcement of beam-to-column dowel joints (T-joints) by studying load-displacement curve with and without reinforcement. However, 2D FE models of timber are best applicable for timber parts with small thickness [7]. Furthermore, in their modeling, they considered timber as an elastic orthotropic material. The elastic orthotropic material model cannot retrace the load-deformation behaviour of timber accurately [7]. In order to take into account the anisotropic nonlinear behaviour of wood, a good agreement was found between numerical simulations and experimental results while considering wood as elastoplastic orthotropic material [7] [8] [9].

In order to evaluate reinforcement in structures, many authors studied the load-displacement curves with and without reinforcement. The reinforcement of walls with densified wood under shear strength was studied in [10]. The experimental results matched well with the numerical simulation. Results showed an increase of the stiffness (strength-to-slip ratio) with reinforced walls. After performing bending tests on glulam beams to predict the load-displacement behaviour in [11], it was found that densified wood used as reinforcement can increase the bending resistance of wood. The efficiency of connections in wood (wood-wood connection and wood-steel connection) was compared in [12] from bending tests. Results from load-displacement curves showed an increase of loads and a reduction of displacements when steel (dowels and plates) is used in the connection.

To assess wood connection systems through testing, two major aspects still require solutions. The first is the development of protocols for long-term loads and repeated loads. The second is the definition of failure for systems developing large deformations before the maximum load [13] [14]. An incremental and iterative method could provide a solution to these aspects for the fact that it enables to describe the state of the structure at each step of load increment. The one which is best known is the Newton-Raphson method.

An analytical model was developed in [15] using the Newton-Raphson method to design plastic structures. Its implementation was adapted for a specific software CEPAO. Besides, this model was useful for steel frame structures. An automatic method was developed in [16] to analyse the (P-Δ) effect using the Newton-Raphson method in steel plane structures. A theoretical model was developed in [17] to perform a nonlinear analysis on a timber beam using the Newton-Raphson method. However, these studies are performed either on steel or on wood. They don't consider both materials. Furthermore, they are not interested in carrying out the effect of steel on the stability of wood structures.

The present work predicted the load-displacement behaviour in a wood structure with bolted wood connection using the Newton-Raphson method numerically implemented in RFEM 5, a finite-element software developed by Dlubal Software Group. On one hand, the beam has been considered without wood connection, on the other hand, the beam has been considered with a bolted wood connection and a slotted-in steel plate. Self-weight and a uniformly applied long-term load have been considered as load cases. Serviceability limits states (SLS) and ultimate limits states (ULS) have also been considered as combinatorics among others. A finite-element software RFEM 5 has been used to implement the model. Results showed that steel can reduce displacement by 20.96%.

2. Materials and Method

2.1. Materials

Tali wood and Fraké wood were selected in this work. **Table 1** presents some physical and mechanical properties of these species, referenced in the Tropix 7.0 database. Tali wood is a dense and emblematic hardwood from the Congo Basin. The colour of the wood varies from orange yellow brown to reddish brown. The colour of Frake wood is light yellow and does not have demarcated sapwood. These species are abundant and can be glued for a structural use. They present a good interest for a glulam use [1]. The differences of densities and elasticity moduli (MOE) should make Tali and Frake, respectively, suitable for external and internal lamellae of the glulam. For this work, we have selected Epoxy as our glue. Its characteristics were set up as presented on **Table 2**.

Table 1. Average and standard values of some physical and mechanical properties of Tali and Frake woods at 12% moisture content [18].

Timber Species	Density (kg/m^3)	Total Tangential Shrinkage (%)	Total Radial Shrinkage (%)	MOE (MPa)	Saturation Fiber Point (%)
Tali	910 ± 80	8.4 ± 1.2	5.1 ± 1.4	19,490 ± 3,224	26
Frake	540 ± 70	6.1 ± 0.9	4.3 ± 1.1	11,750 ± 2,480	28

Table 2. Average characteristics of Epoxy at 23˚C [19].

Type of glue	Relative density (g/cm^3)	MOE (MPa)	Poisson's ratio
Epoxy	1.3299	3355.78	0.43

In this study we have considered the following dimensions of the beam, length: 30 m, width: 100 mm, height: 78 mm. Since our software could not consider more than 3 lamellae, we have set the number of lamellae to 3. The thickness of each lamella has been set to 25 mm, and the thickness of each glue layer was set to 1.5 mm. The characteristics of the bolts will be determined in the method.

2.2. Method

The simulation of the load-displacement (P-Δ) behaviour was made according to the following assumptions:

- Wood is an elastoplastic orthotropic material [7];
- The transverse isotropy is considered, which assumes identical properties in the radial and tangential directions [4] [5];
- Glue is isotropic linearly elastic;
- Bolts are modelled as elastic-perfectly plastic material;
- The hole clearance and the splitting in timber due to tension stresses perpendicular to the grain don't have a significant influence in the load-deformation analysis [20] [21];
- Out-of-plane deformations are not considered;
- The beam is subjected to uniformly applied long-term loads;
- Moisture content is constant;
- Bending strength is dominant in wood connections [22].

In order to determine the characteristics of bolts, we have used the yield theory through Equations (1) to (3) [23]:

$$M_{el} = f_y \frac{\pi d^3}{32} \quad (1)$$

$$M_{pl} = f_y \frac{d^3}{6} \quad (2)$$

$$M_{y,Rk} = 0.3 f_{u,k} d^{2.6} \quad (3)$$

where M_{el} is the elastic moment of bolt, M_{pl} is the plastic moment, f_y is the yield strength, d is the diameter of bolt which is set to 12 mm in this study, $M_{y,Rk}$ is the yield bending moment of bolt and $f_{u,k}$ its tensile strength.

We can express the shear strength $F_{V,Rk}$ of bolt using Equation (4) from Eurocode 5 [23]:

$$F_{V,Rk} = \min \begin{cases} f_h \cdot t \cdot d \\ f_h \cdot t \cdot d \cdot \left[\sqrt{2 + \frac{4 \cdot M_{y,Rk}}{f_h \cdot d \cdot t^2}} - 1 \right] \\ \sqrt{4 \cdot M_{y,Rk} \cdot f_h \cdot d} \end{cases} \quad (4)$$

where f_h is the embedding strength of wood, t is the thickness of wood and d the diameter of bolt. The embedding strength of wood can be expressed from Equation (5) [23]:

$$f_h = 0.082 \times (1 - 0.01 \times d) \times \rho_k \quad (5)$$

where ρ_k is the relative density of wood.

There are two ways to express the ultimate shear strength. According to Eurocode 5 we have Equation (6) [23]:

$$F_{V,Rd} = F_{V,Rk} \cdot \frac{k_{mod}}{\gamma_M} \quad (6)$$

where k_{mod} is the modification factor of wood and γ_M its partial coefficient. The second way to express the ultimate shear strength is Equation (7) from Eurocode 3 [24]:

$$F_{V,Rd} = \frac{\alpha_V \cdot f_{ub} \cdot A}{\gamma_{M2}} \quad (7)$$

where α_V is a coefficient depending on the class resistance of bolt, f_{ub} is the notation of $f_{u,k}$ in Eurocode 3, A is the cross section of bolt and $\gamma_{M2} = 1.25$.

If $F_{V,Ed}$ is the applied load, the number of bolts can be determined from Equation (8) [23]:

$$n = \frac{F_{V,Ed}}{F_{V,Rd}} \quad (8)$$

2.2.1. The Newton-Raphson Method

Algorithms that aim at solving nonlinear problems have become a necessity to develop theoretical models with complex behavior. It becomes essential to have reliable and efficient resolution algorithms. The classical resolution algorithms used in the finite element method are incremental and iterative algorithms, which often have convergence issues related to the existence of limits in terms of loads, displacements or both at the same time. The incremental and iterative method consists of applying gradually a load by increments, and to find for each increment, the structure response. This response is obtained after linearizing the equilibrium equations [25] [26] [27]. The incremental and iterative method commonly used is the Newton-Raphson method. It consists of setting a load increment, and applying for each increment a correction on the equilibrium equations using an iterative process. This correction is done through a tangent stiffness matrix. We can describe this process as follows: a structure is subjected to a total load $\{F\}$, this load is applied step by step. Let's $\{\Delta F\}$ be the load increment. At step $m+1$, load can be expressed from Equation (9):

$$^{m+1}\{F\} = {}^{m}\{F\} + {}^{m+1}\{\Delta F\} \tag{9}$$

The left superscript m indicates the incremental step m. let's $^{m}\{U\}$, $^{m}\{\sigma\}$, $^{m}\{\varepsilon\}$ be our solutions at step m, at step $m+1$, for a load increment $\{\Delta F\}$, we have Equations (10) to (12):

$$^{m+1}\{U\} = {}^{m}\{U\} + \{\Delta U\} \tag{10}$$

$$^{m+1}\{\sigma\} = {}^{m}\{\sigma\} + \{\Delta\sigma\} \tag{11}$$

$$^{m+1}\{F\} = {}^{m+1}\{R\} \tag{12}$$

Equation (12) is the equilibrium between the external nodal loads $^{m+1}\{F\}$ and the internal nodal loads $^{m+1}\{R\}$. But in practice, the two sets of loads are not equal. The difference between them is called residual loads and expressed by Equation (13):

$$\Delta F = {}^{m+1}\{F\} - {}^{m+1}\{R\} \tag{13}$$

These residual loads should be undermined to insure the equilibrium. The Newton-Raphson method uses the tangent stiffness matrix updated at each iteration to correct the equilibrium (see on **Figure 1**).

This method has a rapid convergence, but its main inconvenient is the computing time to update the tangent stiffness matrix at each iteration. This computing time is costly when modelling at large scale and with high degrees of freedom. In order to reduce computing time, we often prefer the modified Newton-Raphson method. This method is identical to the classical Newton-Raphson method except for the fact that, the tangent stiffness matrix remains constant at each increment (see on **Figure 2**).

2.2.2. Modelling and Loading of the Beam Column

First and foremost, we have determined the total weight of the beam taking into account the characteristics of the materials. The beam is made of Tali and glue. The total self-weight stands at 0.078 KN·m^{-1} (see on **Figure 3**). **Figure 4** illustrates the mid-span deflection.

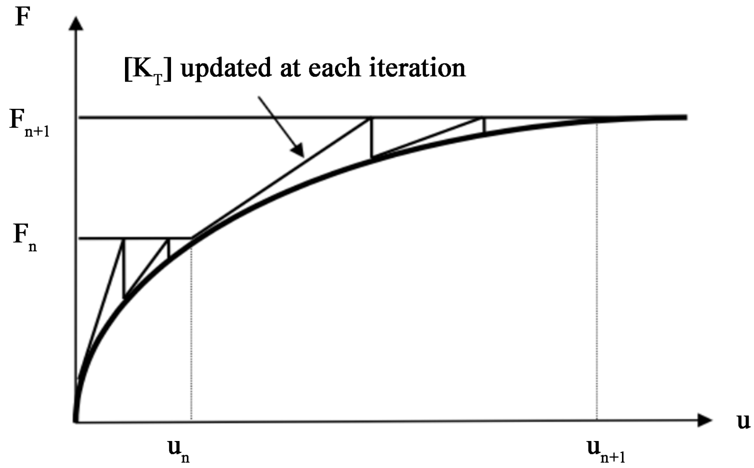

Figure 1. Newton-Raphson method, K_T updated at each iteration.

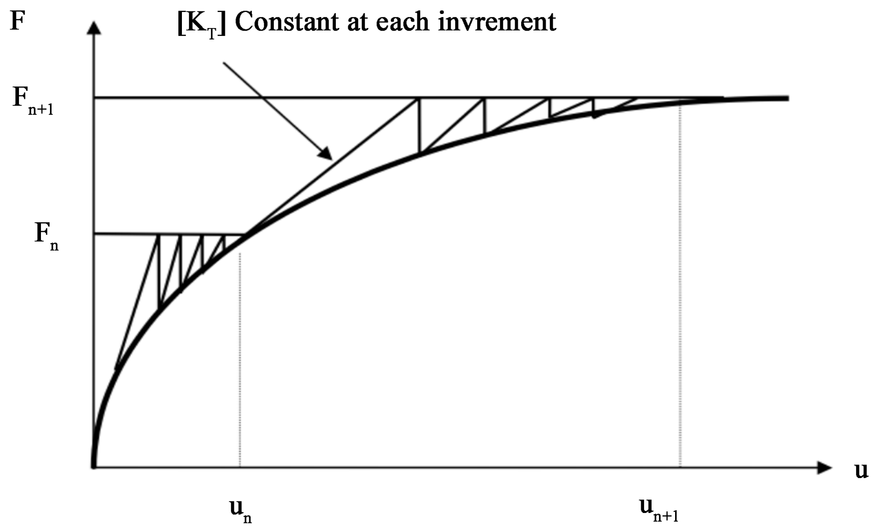

Figure 2. Modified Newton-Raphson method, K_T is constant at each increment.

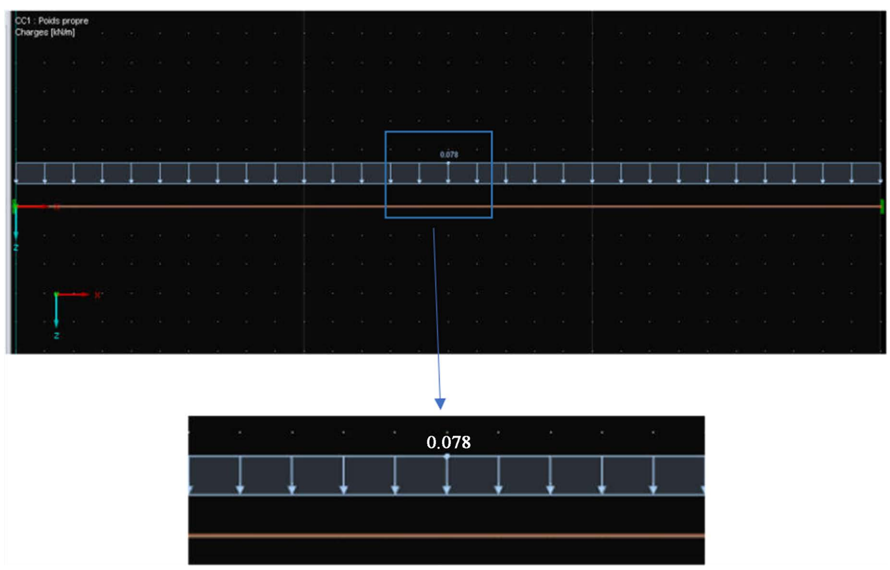

Figure 3. Beam subjected to its self-weight.

The beam is embedded at the two ends. Figure 5 shows one embedded end, and Figure 6 indicates the long-term applied load of 5 KN·m^{-1} on the beam.

The stability check of the bolted wood connection is performed on Figure 7, and Figure 8 shows the top view of the bolted wood connection with a slotted-in steel plate.

A set of 2 loads cases and 5 combinatorics were considered as indicated on Table 3.

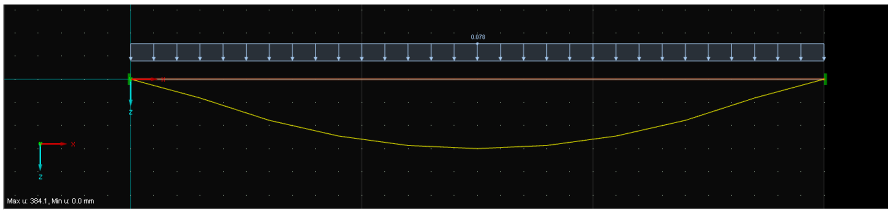

Figure 4. Mid-span deflection.

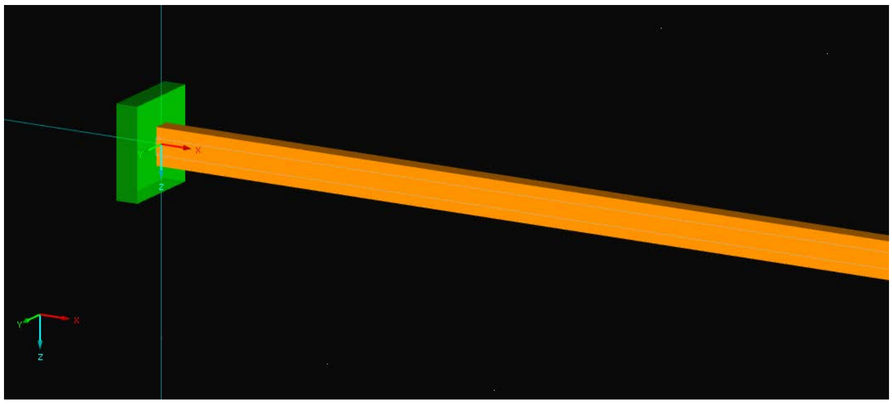

Figure 5. One embedded end of the beam.

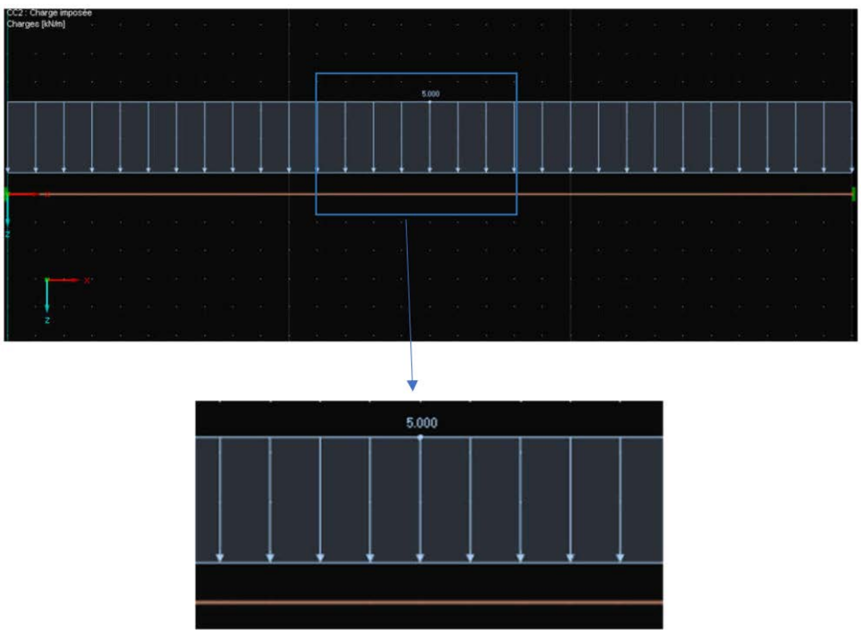

Figure 6. Beam subjected to the long-term applied load.

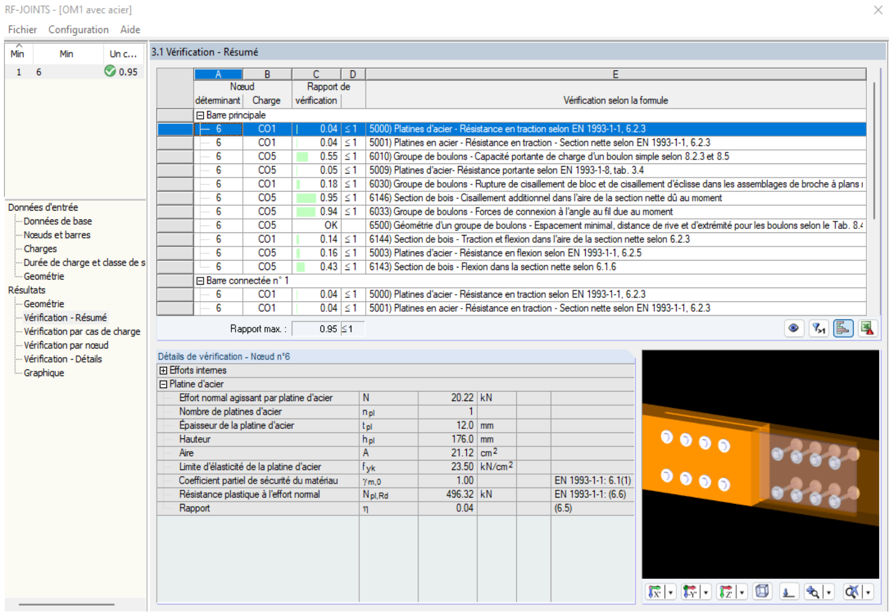

Figure 7. Stability check of the bolted wood connection.

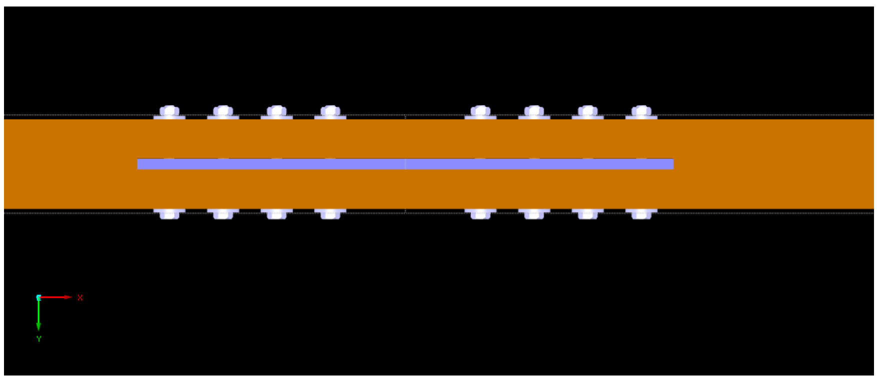

Figure 8. Top view of the bolted wood connection with a slotted-in steel plate.

Table 3. Loads cases and combinatorics considered.

Groups	Names	Description
Loads Cases	CC1	Self-Weight
	CC2	Applied Load
Combinatorics	CO1	1.35 × CC1
	CO2	1.35 × CC1 + 1.5 × CC2 (ULS)
	CO3	CC2
	CO4	1.8 × CC1
	CO5	CC1 + CC2 (SLS)

3. Results and Discussion

3.1. Results

For the self-weight CC1, Figure 9 displays displacements over increments and iterations without bolted wood connection, and with a bolted wood connection. The results obtained in this Figure are found respectively on Table 4 and Table 5.

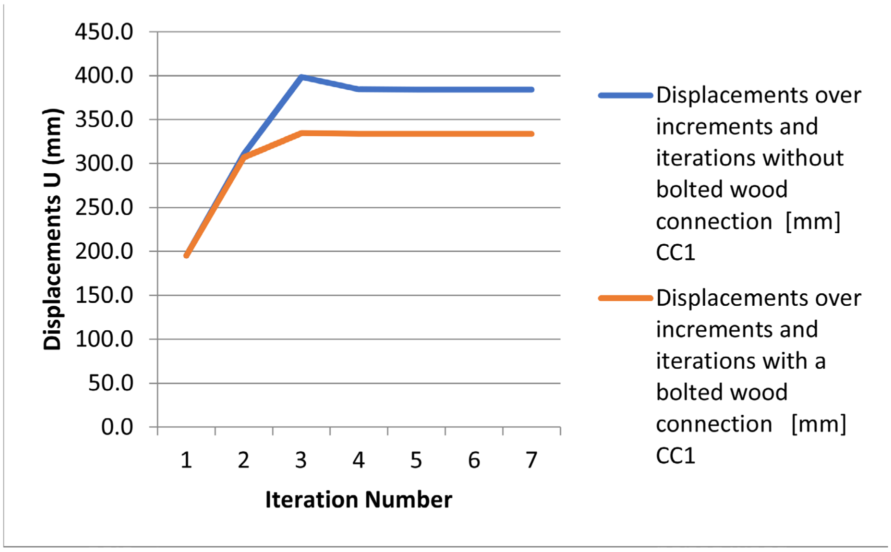

Figure 9. Displacements over increments and iterations with and without bolted wood connection for the self-weight.

Table 4. Results for the self-weight without bolted wood connection.

Increment n°	Iteration n°	Load factor (λ) [−]	Displacement (u) [mm]
1	1	0.030	195.3
1	2	0.309	311.2
1	3	1.000	398.8
1	4	1.000	384.7
1	5	1.000	384.1
1	6	1.000	384.1
1	7	1.000	384.1

Table 5. Results for the self-weight with a bolted wood connection.

Increment n°	Iteration n°	Load factor (λ) [−]	Displacement (u) [mm]
1	1	0.043	195.3
1	2	0.479	307.4
1	3	1.000	334.9
1	4	1.000	333.6
1	5	1.000	333.6
1	6	1.000	333.6

The curves on Figure 9 increase to reach maximum values. These values are maximum displacements. It stands at $u_{max} = 384.1\text{ mm}$ for the self-weight without bolted wood connection (see on Table 4), and $u_{max} = 333.6\text{ mm}$ with bolted wood connection (see on Table 5). The presence of the residual loads can increase these values to $u_{max} = 398.8\text{ mm}$ without bolted wood connection (see on Table 4, iteration n˚3), and $u_{max} = 334.9\text{ mm}$ with bolted wood connection (see on Table 5, iteration n˚3). Displacements are greater for the self-weight without bolted wood connection. This difference stands at $\Delta u_{max} = 50.5\text{ mm}$. It means that the presence of steel has reduced the maximum displacement by 50.5 mm (13.15% of the initial displacement). According to Eurocode 5, especially the standard NF EN 1995-1-1/NA, the maximum deflection W_{fin} caused by the set of loads and creep is $W_{fin} = L/125 = 240\text{ mm}$ (L = 30 m). Compared to the previous values, the gap between this maximum deflection and maximum displacements is 37.5% without bolted wood connection, and 28.06% with bolted wood connection. From iteration n˚1 to iteration n˚2, load factor has been increased by 0.436 (1.02 KN) and displacement has increased by 112.1 mm with bolted wood connection (see on Table 5). The strength-to-displacement ratio stands at 9 N for 1 mm. While, load factor has been increased by 0.279 (0.65 KN) and displacement by 115.9 mm without bolted wood connection (see on Table 4). The strength-to-displacement ratio is rather 5.61 N for 1 mm Thus, by reducing displacements and increasing load factors, steel brought more stability to the structure.

For the long-term load CC2, Figure 10 displays displacements over increments

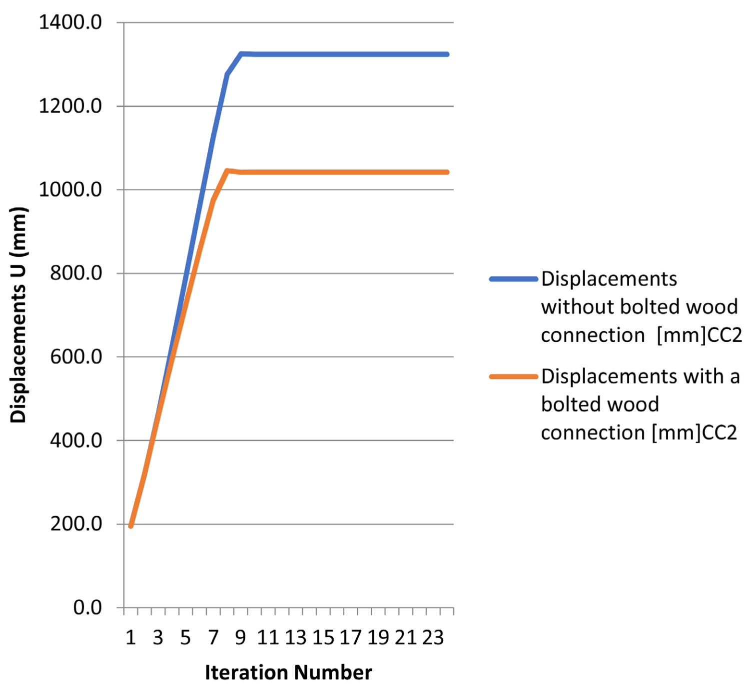

Figure 10. Displacements over increments and iterations with and without bolted wood connection for the applied load CC2.

and iterations without bolted wood connection, and with a bolted wood connection. The results obtained from this Figure are found on Table 6 and Table 7.

On Figure 10, the maximum values are respectively $u_{max} = 1324.1\text{ mm}$ for CC2 without bolted wood connection, and $u_{max} = 1042.5\text{ mm}$ with bolted wood connection (see on Table 6 and Table 7). The difference stands at $\Delta u_{max} = 281.6\text{ mm}$ (21.27% of the initial displacement). This difference is greater than the one obtained for CC1. It means that the more the loads are high, the more steel reduces their displacements. We can also notice that these displacements are greater than the limit W_{fin} provided by Eurocode 5. The gap stands at 81.87% without bolted wood connection, and 76.98% with bolted wood connection. Load factors

Table 6. Results for CC2 without bolted wood connection.

Increment n°	Iteration n°	Load factor (λ) [−]	Displacements (u) [mm]
1	1	0.001	195.3
1	2	0.008	320.0
1	3	0.028	466.2
1	4	0.076	625.5
1	5	0.165	792.2
1	6	0.314	961.7
1	7	0.537	1127.4
1	8	0.837	1276.4
1	9	1.000	1325.4
1	10	1.000	1324.1
1	11	1.000	1324.1
1	12	1.000	1324.1
1	13	1.000	1324.1
1	14	1.000	1324.1
1	15	1.000	1324.1
1	16	1.000	1324.1
1	17	1.000	1324.1
1	18	1.000	1324.1
1	19	1.000	1324.1
1	20	1.000	1324.1
1	21	1.000	1324.1
1	22	1.000	1324.1
1	23	1.000	1324.1
1	24	1.000	1324.1

Table 7. Results for CC2 with bolted wood connection.

Increment n°	Iteration n°	Load factor (λ) [−]	Displacements (u) [mm]
1	1	0.002	195.3
1	2	0.016	321.2
1	3	0.059	461.4
1	4	0.140	595.1
1	5	0.274	726.8
1	6	0.475	855.6
1	7	0.753	976.2
1	8	1.000	1046.3
1	9	1.000	1042.4
1	10	1.000	1042.4
1	11	1.000	1042.4
1	12	1.000	1042.5

are greater and increase faster with bolted wood connection. From iteration n°1 to iteration n°8 it has increased by 0.836 (125.4 KN) without bolted wood connection, and by 0.998 (149.7 KN) with bolted wood connection (see on Table 6 and Table 7). In the meantime, displacements have increased by 1081.1 mm without bolted wood connection (115.99 N for 1 mm), and by 851 mm with bolted wood connection (175.9 N for 1 mm). At iteration n°1, displacements remain the same ($u = 195.3\ \text{mm}$). It means that for very low load factors ($\lambda \leq 0.008$), there is no need to use steel reinforcement. In other words, for loads lesser than $P = 1.2\ \text{KN}$, there is no need to use steel reinforcement.

Figure 11 displays displacements over increments and iterations for the combinatoric CO1 with and without bolted wood connection. The results corresponding to these curves are respectively found on Table 8 and Table 9.

On Figure 11, the curves reach maximum values before stabilizing. These values are respectively $u_{\max} = 466.4\ \text{mm}$ without bolted wood connection and $u_{\max} = 406.3\ \text{mm}$ with bolted wood connection (see on Table 8 and Table 9). Here steel has reduced maximum displacements by $\Delta u_{\max} = 60.1\ \text{mm}$. This difference is greater than the one obtained from self-weight CC1. Indeed, this combinatoric is greater than self-weight (CO1 = 1.35 × CC1). The more displacements are high, the more impact of steel is visible. In other words, the more loads are high, the more bolted wood connection absorbs them. It is the elastic-perfectly plastic character of steel that is highlighted.

For the ULS (CO2 = 1.35 × CC1 + 1.5 × CC2), Figure 12 shows the plot of displacements over increments and iterations with and without bolted wood connection. The results of these curves are found on Table 10 and Table 11, respectively for CO2 without bolted wood connection, and with bolted wood connection.

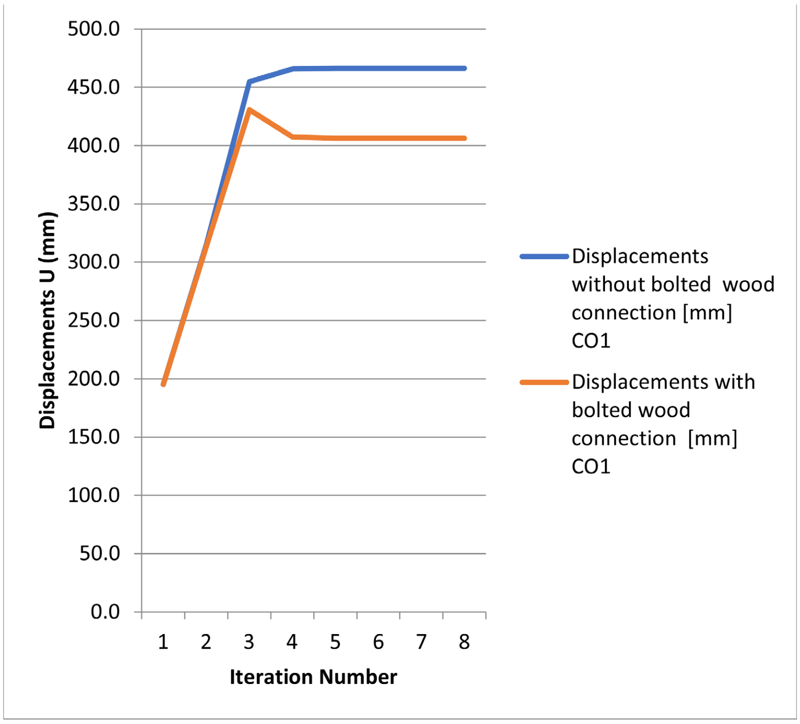

Figure 11. Displacements over increments and iterations for the combinatoric CO1.

Table 8. Results for the combinatoric CO1 without bolted wood connection.

Increments n°	Iteration n°	Load factor (λ) [−]	Displacements (u) [mm]
1	1	0.017	195.3
1	2	0.172	315.2
1	3	0.685	454.9
1	4	1.000	466.0
1	5	1.000	466.4
1	6	1.000	466.4
1	7	1.000	466.4
1	8	1.000	466.4

Table 9. Results for the combinatoric CO1 with bolted wood connection.

Increment n°	Iteration n°	Load factor (λ) [−]	Displacements (u) [mm]
1	1	0.025	195.3
1	2	0.264	313.9
1	3	1.000	430.8
1	4	1.000	407.5
1	5	1.000	406.3
1	6	1.000	406.3
1	7	1.000	406.3

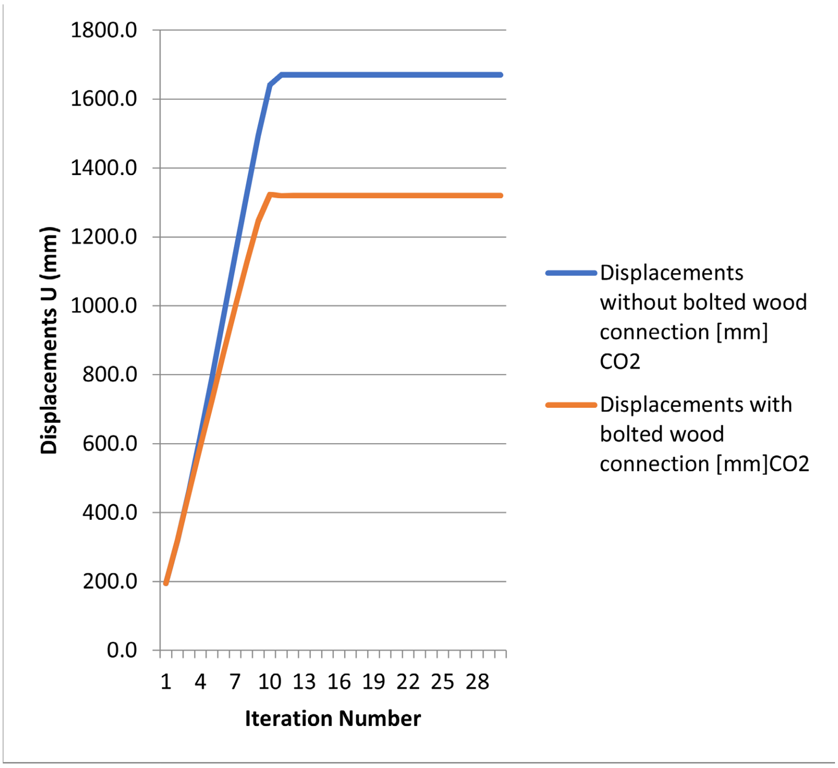

Figure 12. Displacements over increments and iterations for CO2.

Table 10. Results for CO2 without bolted wood connection.

Increments n°	Iteration n°	Load Factor (λ) [−]	Displacements (u) [mm]
1	1	0.000	195.3
1	2	0.004	320.0
1	3	0.014	466.4
1	4	0.038	626.5
1	5	0.083	795.5
1	6	0.158	970.9
1	7	0.274	1149.2
1	8	0.439	1326.2
1	9	0.657	1495.1
1	10	0.917	1641.8
1	11	1.000	1670.6
1	12	1.000	1670.5
1	13	1.000	1670.5
1	14	1.000	1670.4
1	15	1.000	1670.4
1	16	1.000	1670.4

Continued

1	17	1.000	1670.4
1	18	1.000	1670.4
1	19	1.000	1670.4
1	20	1.000	1670.4
1	21	1.000	1670.4
1	22	1.000	1670.4
1	23	1.000	1670.4
1	24	1.000	1670.4
1	25	1.000	1670.4
1	26	1.000	1670.4
1	27	1.000	1670.4
1	28	1.000	1670.4
1	29	1.000	1670.4
1	30	1.000	1670.4

Table 11. Results for CO2 with bolted wood connection.

Increment n°	Iteration n°	Load factor (λ) [−]	Displacement (u) [mm]
1	1	0.001	195.3
1	2	0.008	321.3
1	3	0.029	461.7
1	4	0.069	596.2
1	5	0.135	730.1
1	6	0.234	864.3
1	7	0.375	997.7
1	8	0.563	1127.4
1	9	0.795	1246.7
1	10	1.000	1323.8
1	11	1.000	1320.2
1	12	1.000	1320.2
1	13	1.000	1320.2
1	14	1.000	1320.2
1	15	1.000	1320.2

On **Figure 12**, maximum displacements are respectively $u_{max} = 1670.4\ \text{mm}$ without bolted wood connection, and $u_{max} = 1320.2\ \text{mm}$ with bolted wood connection (see on **Table 10** and **Table 11**). We notice a maximum reduction

$\Delta u_{\max} = 350.2\text{ mm}$ (20.96% of the initial displacement). Indeed, in the ULS loads are greater than any other combinatoric. It is the combinatoric which has the most penalizing effect on the structure. Compared to the limit W_{fin} provided by Eurocode 5, the gap stands at 85.63% without bolted wood connection, and 81.82% with bolted wood connection. While there was no need for using steel in the applied load for $\lambda \leq 0.008$ (1.2 KN), it is advised to use steel when one designs at ULS for $\lambda \geq 0.004$ (912.6 N) (see on **Table 10**). For the structural analysis and design, we can define the plastic resistance value of steel as the intersection between the initial tangent stiffness and the tangent stiffness at the final part of the load-displacement curve (F_y, U_y) [6]. This value is determined at the ULS from the load-displacement curve CO2 with bolted wood connection. In order to make it easier we are going to use the original curve from the software (see on **Figure 13**).

From this curve, the plastic resistance F_y corresponds to the 6.9 iteration. We obtain $F_y = 84.34\text{ KN}$ and $U_y = 1323.8\text{ mm}$. To assess the reinforcement of walls with densified wood under shear strength, the stiffness was defined in [10] as the ratio between the maximum load and the maximum slip. Compared to this present study where bending strength is dominant, we can define the bending stiffness by the ratio between the maximum load and the maximum deflection. From **Table 10** and **Table 11**, the bending stiffness has increased from 0.13 KN·mm^{-1} without bolted wood connection to 0.17 KN·mm^{-1} with bolted wood connection. The bending stiffness has been increased by 32.94%. Since the bending stiffness is proportional to the critical load in [1], the increase of the bending stiffness results to the increase of the critical load by 32.94%. Thus, inducing the increase of the bending resistance by 32.94%.

For the SLS (CO5), **Figure 14** displays the curves of displacements over increments and iterations with and without bolted wood connection. **Table 12** and **Table 13** provide their corresponding results.

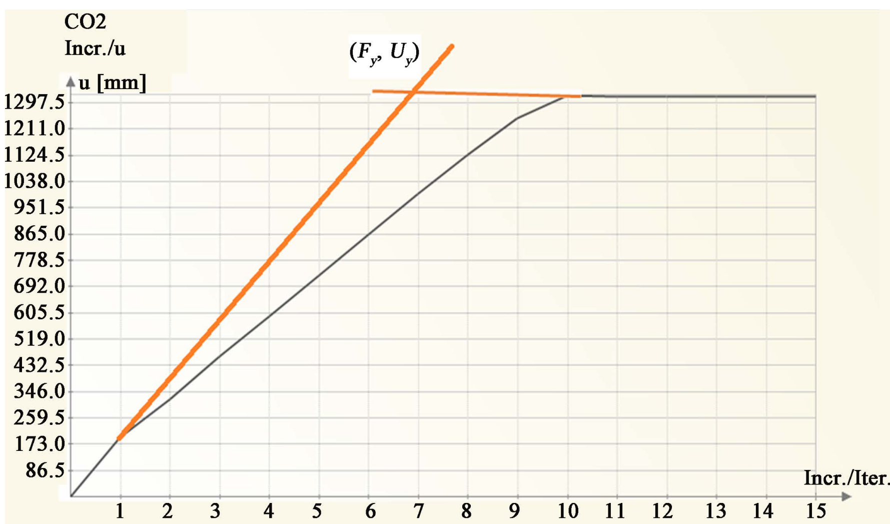

Figure 13. Displacements over increments and iterations for CO2 with bolted wood connection (original curve from the software RFEM5).

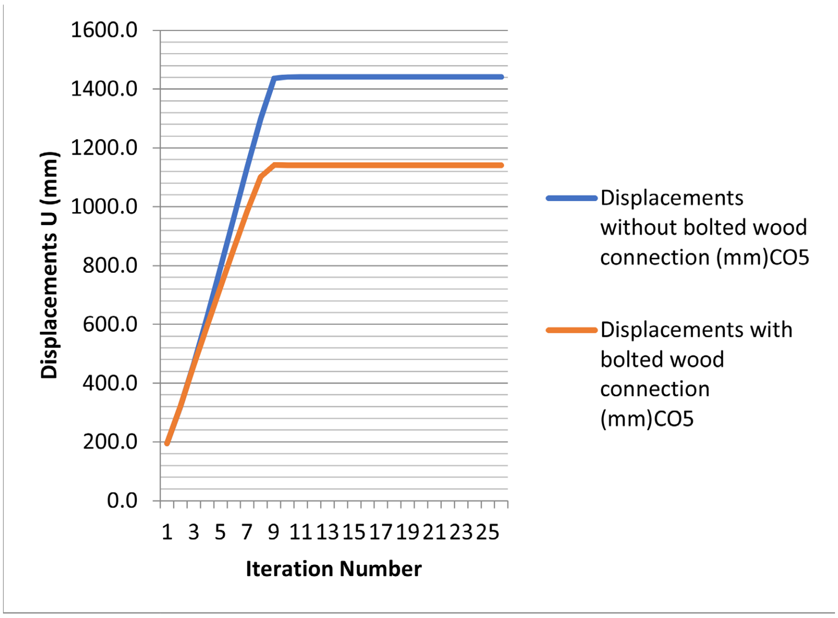

Figure 14. Displacements over increments and iterations for CO5.

Table 12. Results for CO5 without bolted wood connection.

Increments n°	Iteration n°	Load factor (λ) [–]	Displacements (u) [mm]
1	1	0.001	195.3
1	2	0.006	320.0
1	3	0.022	466.3
1	4	0.059	625.9
1	5	0.128	793.7
1	6	0.244	965.9
1	7	0.420	1137.5
1	8	0.665	1300.8
1	9	0.961	1437.7
1	10	1.000	1441.9
1	11	1.000	1441.9
1	12	1.000	1441.9
1	13	1.000	1441.9
1	14	1.000	1441.9
1	15	1.000	1441.9
1	16	1.000	1441.9
1	17	1.000	1441.9
1	18	1.000	1441.9
1	19	1.000	1441.9

Continued

1	20	1.000	1441.9
1	21	1.000	1441.9
1	22	1.000	1441.9
1	23	1.000	1441.9
1	24	1.000	1441.9
1	25	1.000	1441.9
1	26	1.000	1441.9

Table 13. Results for CO5 with bolted wood connection.

Increment n°	Iteration n°	Load factor (λ) [−]	Displacement (u) [mm]
1	1	0.001	195.3
1	2	0.013	321.3
1	3	0.045	461.6
1	4	0.107	595.7
1	5	0.209	728.4
1	6	0.362	859.9
1	7	0.577	987.2
1	8	0.852	1102.6
1	9	1.000	1142.2
1	10	1.000	1141.3
1	11	1.000	1141.3
1	12	1.000	1141.3
1	13	1.000	1141.3
1	14	1.000	1141.4

The maximum displacements are respectively $u_{\max} = 1441.9\ \text{mm}$ mm and $u_{\max} = 1141.4\ \text{mm}$. Here the difference is $\Delta u_{\max} = 300.5\ \text{mm}$ (20.84% of the initial displacement). Displacements are lower than the ones obtained from ULS. In order to ensure the safety of the structure, it is advised to use steel reinforcement for load factors $\lambda \geq 0.006$ (914 N) (see on Table 12 and Table 13). The SLS are used to limit deformations in the structure. During the design process, one should make sure that the value of the mid-span deflection caused by the set of loads applied to the structure remains lower than the limit value.

3.2. Discussion

The model developed in this study could find applications in frameworks, bridges and any structure subjected to high bending strength, where it is important to undermine deformations which can lead to instabilities. For wood beams subjected to bending strength, checking deformations at the SLS is the most important criterion for structural analysis and design [23]. This study enables to predict load-displacement (P-Δ) behaviour in structures subjected to uniformly be applied long-term loads, which is difficult to carry out through testing. The elastoplastic steel properties provide good estimates of load-displacement [28]. Mechanical properties of wood and glue used for the simulation in the software are realistic and obtained from various tests (see on **Table 1** and **Table 2**). Realistic characteristics of steel were used as inputs of the model, since they were drawn from Eurocode 3. The bi-linear trends of load-displacement curves obtained are confirmed by authors such as in [5] [7] and [28]. Knowing the load-displacement behaviour of the structure helps designers reduce costs of construction. Indeed, they are able to know when to use steel reinforcements that are very costly.

Moreover, in the literature it is difficult to find investigations about load-displacement behaviour on large span structures made of tropical hardwood species. Most of studies are dealing with small size structures made of softwoods. For instance, load-displacement behaviour was studied in [12] on a 1200 mm length beam with and without bolted wood connection. They obtained from bending tests approximately 6000 N for 40 mm displacement without steel and 6000 N for 20 mm with steel. In this present study, after performing a linear interpolation from **Figure 11**, **Table 6** and **Table 7**, 6000 N corresponds to 505.9 mm displacement without steel and 399.45 mm with steel. This significant gap could be explained by the differences in the sizes of beams, wood nature and the characteristics of bolts. The plastic resistance obtained in [6] was $F_y = 86.1\ \text{KN}$. In this present study, the plastic resistance is $F_y = 84.34\ \text{KN}$. This slight difference could be explained by the fact that in their work, they have used dowels with class resistance 4.8 which means that the nominal yield and ultimate tensile strength are respectively equal to 320 MPa and 400 MPa [24]. While in this study, class resistance of bolts was set to 4.6 which means that the nominal yield and ultimate tensile strength are respectively equal to 240 MPa and 400 MPa [24].

Conducting experimental investigations on large span structural product would be difficult. Indeed, the process is a priori time-consuming and expensive. For these reasons, the present paper is devoted to modelling by using a 3D FE nonlinear analysis. FE analysis is suited for modelling and evaluating parallel and perpendicular to the grain loading of wood with bolted wood connections [28]. That is the reason why many authors used 3D FE models to predict load-displacement behaviour in timber with bolted wood connections [5] [6] [9] [28].

The iterative Newton-Raphson method was used in [16] to study the nonlinear behaviour of a large span steel frame structure (10 m). A load of 45 tons was uniformly step by step applied to the structure. Their simulation was performed through a CEPAO program. They carried out loads versus displacements curves considering steel as elastic-perfectly plastic material as we did in this work. The trends of the curves were the same as we obtained in this work. The elasto-plastic analysis done in their work revealed that the curves stabilize after a load factor $\lambda = 0.754$ as on **Table 5**, **Table 7**, **Table 9**, **Table 11** and **Table 13** with bolted wood connection, and displacements can go beyond 30 cm. Reference [29] simulated the nonlinear behaviour of a large span glulam beam using the Newton-Raphson method. The beam length was set to 8000 mm and the dimensions of the cross section 200 × 1000 mm^2. Here the tangent stiffness matrix was analytically calculated before being implemented in a MATLAB code. Since the length was smaller than the one used in this present work (30 m), there were less nodes, thus, less nonlinear equations to resolve. This made it possible to calculate analytically the tangent stiffness matrix. In this present work, the tangent stiffness matrix was numerically computed by the software during the simulation. Besides, their nonlinear study was also numerically performed through the step-by-step iterative Newton-Raphson method. Instead of carrying out loads versus displacements curves as we did in this work, they were interested in carrying out loads versus warping angles curves. Results matched well with the ones obtained from the analytical Euler method. Several other authors as in [30] [31] and [32] successfully performed a numerical nonlinear analysis on large span glulam beam columns using the iterative Newton-Raphson method. In most of these cases, a uniform load was step by step applied to the beam. Their works proved the efficiency of the Newton-Raphson method compared to the classical finite element method.

However, this study focused on the nonlinear analysis of the load-displacement behaviour without predicting failure. The stability check for bolts was performed in a different section of the RFEM 5 software called RF-JOINTS (see on **Figure 7**). In order to enable the software to run the simulation, we had to select a load that meets stability conditions for both wood and steel. This made it difficult to predict failure for both materials despite the lack of accuracy in this investigation [28]. Geometrical imperfections due to the curvature of the beam-column (initial out of straightness) were not considered in this work. Such imperfections may create an additional bending moment along the axis of the beam, thus perturbing the loading of the glulam beam [1]. Moreover, the study was carried out with the assumption that the constant climate in the wood moisture content was 12%. The natural climate condition, corresponding to the exposure environment of these beams, generally varies, thus inducing some mechano-sorptive effects in wood which may be characterized by more important deformations.

4. Conclusion

In order to analyse the impact of steel, a nonlinear analysis has been performed by the Newton-Raphson method. This method has the advantage to be easily implemented in finite element software as RFEM 5. Results showed that reduction of displacements can reach up to 350.2 mm (20.96% of the initial displacement). The maximum deflection can reach up to 1670.4 mm for hardwoods while the one provided by Eurocode 5 for softwoods with the same size is 240 mm, the gap stands at 85.63%. For applied loads lesser than $P = 1.2\ \text{KN}$, there is no need to use steel reinforcement. At serviceability limits states, it is advised to use steel reinforcement for load factors $\lambda \geq 0.006$ (914 N). While at ultimate limits states, care should be taken for $\lambda \geq 0.004$ (912.6 N). The plastic resistance of steel can increase the bending resistance of wood by 32.94%. Applying these results in real design cases could help designers undermine deformations and reduce costs of construction by using less steel. Further studies, focusing on experimental investigations in natural tropical and temperate climates, will be achieved to enrich the model proposed in this work. We intend to quantify the mechano-sorptive effects that may occur under these climates to improve the prediction of load-displacement behaviour.

Acknowledgements

We thank the reviewers and editors for their comments for improving the quality of the paper.

Conflicts of Interest

The authors declare no conflicts of interest regarding the publication of this paper.

References

[1] Ourmama, M., Oum Lissouck, R. and Ayina Ohandja, L.M. (2021) Influence of Mixing Tropical Timber Species and Material Heterogeneities on the Long-Term Stability of Slender Glulam Beam Columns. *Wood Material Science & Engineering*, **17**, 918-928. https://doi.org/10.1080/17480272.2021.1977695

[2] Bellassen, V. and Luyssaert, S. (2014) Carbon Sequestration: Managing Forests in Uncertain Times. *Nature*, **506**, 153-155. https://doi.org/10.1038/506153a

[3] Xu, B. (2009) Modélisation du Comportement Mécanique D'assemblages Bois Avec Prise en Compte de Critères de Rupture [Numerical Modelling of the Behaviour of Timber Connections Considering the Damage Evolution]. Ph.D. Dissertation, Blaise-Pascal-Clermont II University, Clermont-Ferrand.

[4] Dias, A.M.P.G., Van de Kuilen, J.W., Lopes, S. and Cruz, H. (2007) A Non-Linear 3D FEM Model to Simulate Timber-Concrete Joints. *Advances in Engineering Software*, **38**, 522-530. https://doi.org/10.1016/j.advengsoft.2006.08.024

[5] Patton-Mallory, M., Cramer, S.M. and Pellicane, P.J. (1997) Nonlinear Material Models for Analysis of Bolted Wood Connections. *Journal of Structural Engineering*, **123**, 1063-1070. https://doi.org/10.1061/(ASCE)0733-9445(1997)123:8(1063)

[6] Bouchaır, A., Racher, P. and Bocquet, J.F. (2007) Analysis of Dowelled Timber to Timber Moment Resisting Joints. *Materials and Structures*, **40**, 1127-1141. https://doi.org/10.1617/s11527-006-9210-0

[7] Eslami, H., Jayasinghe, L.B. and Waldmann, D. (2021) Nonlinear Three-Dimensional Anisotropic Material Model for Failure Analysis of Timber. *Engineering Failure Analysis*, **130**, Article ID: 105764. https://doi.org/10.1016/j.engfailanal.2021.105764

[8] Kharouf, N., McClure, G. and Smith, I. (2003) Elasto-Plastic Modelling of Wood Bolted Connections. *Computers & Structures*, **81**, 8-11. https://doi.org/10.1016/S0045-7949(02)00482-0

[9] Sawata, K. and Yasumura, M. (2003) Estimation of Yield and Ultimate Strengths of Bolted Timber Joints by Nonlinear Analysis and Yield Theory. *Journal of Wood Science*, **49**, 383-391. https://doi.org/10.1007/s10086-002-0497-3

[10] Hassel, I., Berard, P. and Komatsu, K. (2008) Development of Wooden Block Shear Wall—Improvement of Stiffness by Utilizing Elements of Densified Wood. *Holzforschung*, **62**, 584-590. https://doi.org/10.1515/HF.2008.091

[11] Anshari, B., Guan, Z., Komatsu, K., Kitamori, A. and Jung, K. (2010) Explore Novel Ways to Strengthen Glulam Beams by Using Compressed Japanese Cedar. *World Conference on Timber Engineering*, Riva del Garda, 20-24 June 2010, 20-24.

[12] Mehra, S., O'Ceallaigh, C., Hamid-Lakzaeian, F. and Guan, Z. (2018) Evaluation of the Structural Behaviour of Beam-Beam Connection Systems Using Compressed Wood Dowels and Plates. *World Conference on Timber Engineering*, Seoul, 20-23 August 2018, 20-23.

[13] Aune, P. and Patton-Mallory, M. (1986) Lateral Load-Bearing Capacity of Nailed Joints Based on the Yield Theory: Experimental Verification Forest Service. Forest Products Laboratory, Research Paper FPL 470, 29 p.

[14] Larsen, H. (1994) Connections and Joints. *Proceedings of Pacific Timber Engineering Conference*, Gold Coast, 11-15 July 1994, 60-66.

[15] Hung, N.D. and De Saxcé, G. (1981) Analyse et Dimensionnement Plastique des Structures a Barres Dans Les Conditions de StabilitE [Analysis and Plastic Designing of Bar Structures under Stable Conditions]. Metallic Construction No. 3-1981, University of Liège, Liège.

[16] De Saxce, G. and Ayina Ohandja, L.M. (1985) Une Méthode Automatique de Calcul de L'effet (P-Delta) Pour L'analyse Pas-À-Pas des Ossatures Planes [An Automatic Method for Computing the (P-Delta) Effect to Analyse Step-by-Step In-Plane Frameworks]. Metallic Construction No. 3-1985, University of Liège, Liège.

[17] Bikanda, L.E., Oum Lissouck, R., Mvogo, J.K., Angouah Massaga, J.M. and Ayina Ohandja, L.M. (2018) Simulation of the Geometric Instability of Wood Beams by Using the Newton Raphson Method. *International Journal of Science and Research* (*IJSR*), **7**, 1474-1482.

[18] CIRAD (2011) Centre de Cooperation Internationale de Recherche Agricole Pour le Developpement [International Cooperation Centre of Agricultural Research for Development, French] Tropix 7.0. Synthese des Caracteristiques Technologiques de 245 Essences Tropicales. Montpellier.

[19] Bart, A. (2009) Experimental Characterization of a Structural Adhesive Joint and a Composite Material with Randomly Oriented Short Fibers. Master's Thesis, University of Sherbrooke, Québec.

[20] Lopes, S., Cruz, H. and Dias, A. (2003) Trial Tests on Timber-Concrete Connections. 2*nd International Symposium on Building Pathology*, *Durability and Rehabilitation*, Lisbon, 6-8 November 2003, 211-220.

[21] Dias, A.M.P.G. (2005) Mechanical Behaviour of Timber-Concrete Joints. Ph.D. Thesis, Delft University of Technology, Delft.

[22] Laplanche, K. (2006) Etude du Comportement au Feu des Assemblages de Structures Bois: Approche Expérimentale et Modélisation [Study of Wood Connections Behaviour Under Fire: Experimental Approach and Modelling, French]. Ph.D. Thesis, Blaise Pascal-Clermont II University, Clermont-Ferrand.

[23] Benoit, Y., Legrand, B. and Tastet, V. (2008) Eurocode 5, Calcul des Structures en Bois. Eyrolles-Afnor, Paris. (In French)

[24] Morel, J. (2005) Eurocode 3, Calcul des Structures Métalliques. Eyrolles, Paris. (In French)

[25] Zarhouni, H. (1998) Methode Asymptotique Numerique Pour Les Coques en Grandes Rotations. Ph.D. Thesis, University of Metz, Metz. (In French)

[26] Dureisseix, D. (2008) Méthodes Numériques Appliquées à la Conception Par Éléments Finis [Numerical Methods Applied to Design with Finite Elements, French]. Master's Thesis, University of Montpellier, Montpellier.

[27] Duval, M. (2016) Apports du Couplage Non-Intrusif en Mecanique Non-Lineaire des Structures. Ph.D. Thesis, University of Toulouse, Toulouse. (In French)

[28] Moses, D.M. and Prion, H.G.L. (2003) A Three-Dimensional Model for Bolted Connections in Wood. *Canadian Journal of Civil Engineering*, **30**, 555-567. https://doi.org/10.1139/l03-009

[29] Bikanda, L.E., Oum Lissouck, R., Angouah Massaga, M.J. and Ayina Ohandja, L.M. (2023) Non-Linear Analysis of the Flexural-Torsional Stability of Slender Tropical Glulam Beams. *The Journal of Strain Analysis for Engineering Design*, **59**, 108-122. https://doi.org/10.1177/03093247231204645

[30] Ait-Mokhtar, A., El-Ghaoui, A. and Ouled-Ali, A. (2013) Numerical Analysis of Large Span Glulam Beams. *Journal of Structural Engineering*, **139**, 2893-2902.

[31] Ben-Moussa, M.A., El-Ghaoui, A. and Ouled-Ali, A. (2017) Numerical Study of Large Span Glulam Beams Subjected to Locally Applied Loads. *Construction and Building Materials*, **132**, 112-122.

[32] Ben-Moussa, M.A., El-Ghaoui, A. and Ouled-Ali, A. (2018) Méthode Numérique de Newton-Raphson Pour L'étude des Bois Lamellés Collés de Grande Portée [The Newton-Raphson Numerical Method for the Study of Large Span Glulam Beams]. *Revue des Matériaux*, **63**, 158-164. (In French)